Cell PRESS
Structure
Article

POT1-TPP1 Regulates Telomeric Overhang Structural Dynamics

Helen Hwang,[1,2] Noah Buncher,[5] Patricia L. Opresko,[5] and Sua Myong[1,3,4,*]
[1]Bioengineering Department
[2]Medical Scholars Program
[3]Institute for Genomic Biology
[4]Center of Physics for Living Cells
University of Illinois, Urbana, IL 61801, USA
[5]Department of Environmental and Occupational Health, University of Pittsburgh, Pittsburgh, PA 15260, USA
*Correspondence: smyong@illinois.edu
http://dx.doi.org/10.1016/j.str.2012.08.018

SUMMARY

Human telomeres possess a single-stranded DNA (ssDNA) overhang of TTAGGG repeats, which can self-fold into a G-quadruplex structure. POT1 binds specifically to the telomeric overhang and partners with TPP1 to regulate telomere lengthening and capping, although the mechanism remains elusive. Here, we show that POT1 binds stably to folded telomeric G-quadruplex DNA in a sequential manner, one oligonucleotide/oligosaccharide binding fold at a time. POT1 binds from 3′ to 5′, thereby unfolding the G-quadruplex in a stepwise manner. In contrast, the POT1-TPP1 complex induces a continuous folding and unfolding of the G-quadruplex. We demonstrate that POT1-TPP1 slides back and forth on telomeric DNA and also on a mutant telomeric DNA to which POT1 cannot bind alone. The sliding motion is specific to POT1-TPP1, as POT1 and ssDNA binding protein gp32 cannot recapitulate this activity. Our results reveal fundamental molecular steps and dynamics involved in telomere structure regulation.

INTRODUCTION

Telomeres are nucleoprotein DNA structures that cap the ends of linear chromosomes to prevent degradation and chromosome end-to-end fusions caused by the inappropriate activity of DNA nucleases and repair enzymes (d'Adda di Fagagna et al., 2003). Telomeres are essential for genome stability and cell survival, and defects in telomere maintenance correlate with human disease including cancers (Armanios et al., 2009). Telomeric ends in most eukaryotes consist of repeat sequences with guanine base runs on the 3′ single-stranded DNA (ssDNA). In humans, the telomeric overhang consists of 50–200 nucleotides of tandem TTAGGG repeats, which serves as the substrate for telomere elongation by telomerase (Makarov et al., 1997). The chemical nature of the G-rich repeats allows for the ssDNA overhang to fold into G-quadruplex structure that consist of three tetrads of four guanines interacting via Hoogsteen base pairing (Gilbert and Feigon, 1999; Neidle and Parkinson, 2003; Sundquist and Klug, 1989; Williamson et al., 1989).

In humans, the telomeric overhang is bound by POT1 and TPP1, which are the homologs of ciliate proteins TEBPα and TEBPβ, respectively (Baumann and Cech, 2001; Wang et al., 2007; Xin et al., 2007). POT1 binds single-stranded TTAGG GTTAG sequence and prevents the inappropriate activation of Ataxia-telangiectasia-mutated and Rad3-related kinase at the 3′ telomeric overhang to ensure that the chromosome end is not recognized as DNA damage (Denchi and de Lange, 2007). Partial loss or reduction of the 3′ telomere overhang elicits a DNA damage response at telomeres in G1 phase of cell cycle (Hockemeyer et al., 2005), indicating a role of POT1 in protecting the telomere end. TPP1 increases the affinity of POT1 for DNA by 10-fold (Wang et al., 2007; Xin et al., 2007) and also recruits telomerase in vivo (Abreu et al., 2010). RNA interference silencing of either POT1 or TPP1 induces telomere lengthening and chromosomal instability (Kelleher et al., 2005; Liu et al., 2004; Veldman et al., 2004; Ye et al., 2004), clearly indicating their role in regulating telomerase access to the overhang. In addition, TPP1 partners with POT1 to enhance telomerase processivity in vitro (Wang et al., 2007). However, unlike the ciliate counter parts, little is known regarding TPP1 or POT1 modulation of telomeric DNA structure and G-quadruplex dynamics.

Using single molecule fluorescence assays, we determined the molecular mechanism involved in the interaction between the telomere overhang and its binding proteins, POT1 and the POT1-TPP1 complex. We find that a POT1 monomer binds the telomeric overhang in two successive steps whereby one step likely represents an individual oligonucleotide/oligosaccharide binding (OB) fold engaging with one repeat sequence. This results in a sequential unfolding of the G-quadruplex in four steps by two POT1 monomers. We also demonstrate that the POT1 binding direction is 3′ to 5′ with respect to the DNA overhang substrate. Surprisingly, the POT1-TPP1 complex exhibits a highly dynamic sliding movement back and forth on the telomeric overhang, which induces continuous unfolding and refolding of the G-quaduplex. The sliding activity we demonstrate here may provide a mechanistic basis for how POT1-TPP1 serves to enhance telomerase processivity (Wang et al., 2007).

RESULTS

POT1 Binds the Telomeric Overhang Sequentially One OB Fold at a Time

The structure of POT1 bound to telomeric DNA reveals extensive contact between the OB folds of POT1 and the 10 nucleotide binding sequence, TTAGGGTTAG. OB1 tightly engages with the TTAGGG and OB2 binds the 3′-terminal TTAG nucleotides, which induces a sharp 90° kink in the DNA backbone at the interface between the two OB domains (Lei et al., 2004). We asked if POT1 can bind the telomeric overhang prefolded in a G-quadruplex. We prepared a 3′ overhang substrate of the sequence $(TTAGGG)_4$, termed "G4" (Table 1), labeled with two fluorescent dyes, Cy3 and Cy5, at both extremities of the ssDNA for measuring fluorescence resonance energy transfer (FRET). As a molecular ruler, FRET reports on the folding status of the DNA since the donor Cy3 dye will be closer to the acceptor Cy5 dye in compact conformations to yield a higher FRET compared to unfolded forms. We added POT1 (100 nM) to the G4 FRET construct (Figure 1A) in 150 mM NaCl; a condition in which G4 exists in one folded conformation (Figures S1A and S1B available online). G4 contains two POT1 binding sites as marked in gray shadow (Figure 1B, top). POT1 binding to G4 resulted in a stepwise FRET decrease (Figure 1C, top). We observed four steps of FRET decrease in the majority of single molecule traces, which is also presented as a transition density plot (TDP) built from over 200 data points (Figure 1D, top). The TDP is formed by plotting FRET before transition and FRET after transition on y- and x axis, respectively. One cluster represents one FRET transition corresponding to one binding or dissociation event whereby binding and dissociation events are plotted in the upper and lower half triangles, respectively (Figure 1D). The POT1 binding to G4 shows four steps of monotonic FRET decrease, indicating successive four-step binding without dissociation. The four steps observed for two monomer binding sites suggest that one POT1 monomer binds in two steps, likely due to the two OB folds binding sequentially. The binding is stable over time as illustrated by the low FRET peak shown in FRET histogram taken at 10–20 min after the protein addition (Figures S1C–S1E).

To further test if the stepwise binding of POT1 occurs one OB fold at a time, we shortened the constructs to create G3 and G2 with three and two TTAGGG repeats, respectively (Figure 1B). G3 provides one and a half POT1 binding site whereas G2 only allows one monomer binding. We note that G3 and G2 are not expected to form higher order structures, yet FRET is 0.7−0.8 due to the ion induced conformational flexibility of ssDNA, which depends on the ssDNA length (Murphy et al., 2004). According to the same study, the length corresponding to G4 (24 nt) should yield a 0.5 FRET. Therefore, the high FRET (0.8) we obtained for G4 above likely arises from the formation of G-quadruplex, whereas the high FRET observed for G3 and G2 results from the short ssDNA tail length. Under the same POT1 binding conditions as the G4 construct, we obtained three and two steps of FRET decrease for the G3 and G2, respectively (Figures 1C and 1D). This is consistent with the interpretation that one POT1 monomer binds in two steps. We reasoned that if the stepwise change in FRET arises from individual OB fold association with the DNA, then the dwell time of the first step (δt1), which represents the initial POT1 binding, but not the second step (δt2), which involves the second OB domain binding, should depend on the protein concentration. To test this, we varied POT1 concentration from 25 to 125 nM and collected dwell times corresponding to the first (δt1) and the second step (δt2) of FRET decrease (from 75 molecules) as denoted in Figure 1C. As predicted, the dwell time shows the expected concentration dependence for the first step, i.e more rapid binding at higher POT1 concentrations, but not for the second step, which remains constant regardless of the POT1 concentration (Figure 1E). This result supports the conclusion that POT1 monomer binds in two successive steps, one OB fold at a time. To further test the individual OB fold binding, we prepared FRET-DNA constructs with targeted mutations. OB1 mutant (TTTTTT TTAG) and OB2 mutant (TTAGGG TTTT) DNA constructs (mutated sequence is underlined) were designed to perturb the binding of OB1 and OB2, respectively (Figure S1G). OB1 mutant shows FRET fluctuation indicating an unstable binding of the OB2

Table 1. List of DNA Oligonucleotides

	Sequence Name 3′Cy3 Sequence
G2	TGG CGA CGG CAG CGA GGC TTA GGG TTA GGG /3′Cy3/
G3	TGG CGA CGG CAG CGA GGC TTA GGG TTA GGG TTA GGG /3′Cy3/
G3 TTAG	TGG CGA CGG CAG CGA GGC TTA GGG TTA GGG TTA GGG TTA G /3′Cy3/
G4	TGG CGA CGG CAG CGA GGC TTA GGG TTA GGG TTA GGG TTA GGG /3′Cy3/
G4 (18 nt Cy3)	TGG CGA CGG CAG CGA GGC TTA GGG TTA GGG TTA GGG /iCy3/ TTA GGG
G4 (12 nt Cy3)	TGG CGA CGG CAG CGA GGC TTA GGG TTA GGG /iCy3/ TTA GGG TTA GGG
G4 (6 nt Cy3)	TGG CGA CGG CAG CGA GGC TTA GGG /iCy3/ TTA GGG TTA GGG TTA GGG
G4 (0 nt)	TGG CGA CGG CAG CGA GGC TTA GGG TTA GGG TTA GGG TTA GGG
OB1OB2	TGG CGA CGG CAG CGA GGC TTA GGG TTA G/3′Cy3/
OB1 mutant	TGG CGA CGG CAG CGA GGC TTT TTT TTA G/3′Cy3/
OB2 mutant	TGG CGA CGG CAG CGA GGC TTA GGG TTT T/3′Cy3/
G2mut2	TGG CGA CGG CAG CGA GGC TTA GGG TTA GGG TTT GGC TTT GGC /3′Cy3/
G2mut4	TGG CGA CGG CAG CGA GGC TTA GGG TTA GGG TTT GGC TTT GGC TTT GGC TTT GGC /3′Cy3/
T25	TGG CGA CGG CAG CGA GGC $(T)_{25}$/3′Cy3/
	Sequence Name 3′ Biotin Sequence
Cy5 18 nt	/5′Cy5/GCC TCG CTG CCG TCG CCA /3′Bio/(annealed to all the 3′ Cy3 sequence listed above)
Cy3 18 nt	/5′Cy3/GCC TCG CTG CCG TCG CCA /3′Bio/
Unlabelled strand	GCC TCG CTG CCG TCG CCA /3′Bio/ (annealed to Cy3-G4 sequences, mutants, and T25 listed above)

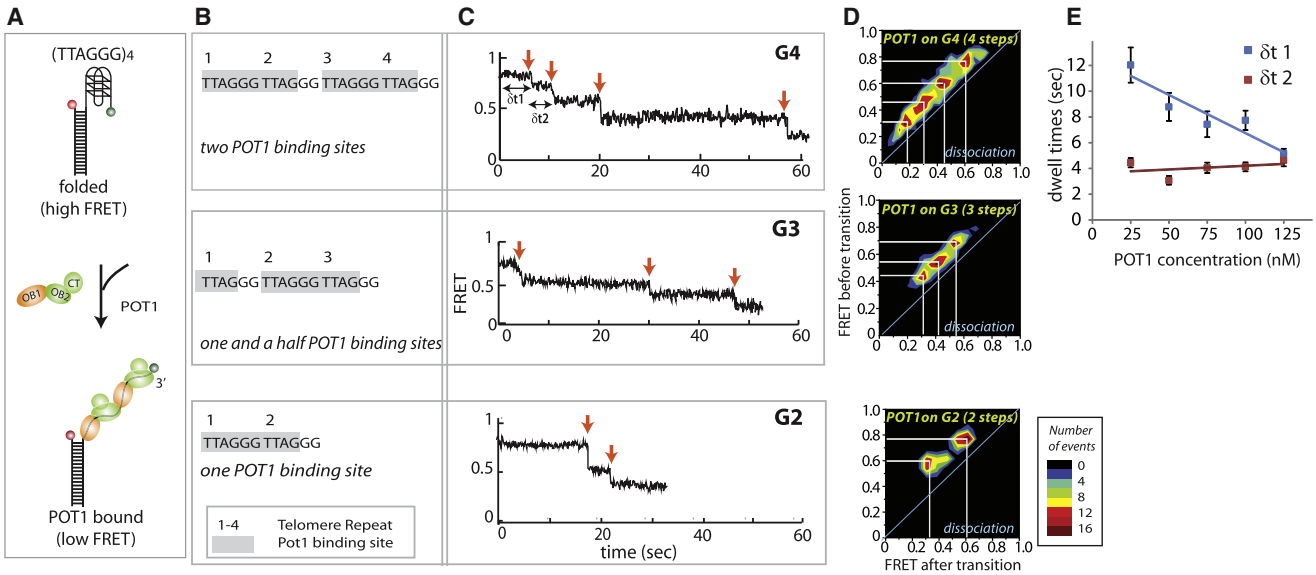

Figure 1. POT1 Binds a Telomeric Overhang One OB Fold at a Time

(A) Schematic of the G4 DNA construct. The strand with four TTAGGG repeats was attached to a single molecule surface by annealing a complementary biotinylated strand to form a duplex. G-quadruplex folding induces high FRET between Cy3 (green) and Cy5 (red) at both ends of the ssDNA.

(B) Telomeric repeats for G4, G3, and G2 with POT1 binding sites marked in gray.

(C) Single molecule traces of POT1 binding to G4, G3, and G2 show four, three, and two steps of FRET decrease (arrow), respectively.

(D) Transition density plots are built from the FRET value before transition in the y axis and the FRET value after transition in the x axis.

(E) Dwell times taken from the first (δt1) and second step (δt2) of FRET decrease obtained from the G4 construct with variable POT1 concentrations.

See also Figure S1. Error bars indicate the SEM.

domain whereas the OB2 mutant shows only one step FRET decrease reflecting a stable binding of the OB1 domain (Figures S1H and S1I). This is consistent with the crystal structure that shows extensive contact between OB1 and TTAGGG bases whereas OB2 shows much fewer contacts with the TTAG base (Lei et al., 2004). This data agrees well with the dwell time analysis (Figure 1E) and further supports our model that POT1 binds one OB fold at a time.

POT1 Binds in 3′ to 5′ Direction

Next, we asked if POT1 binding initiates from the 3′ end or from the duplex junction. We prepared two alternate substrates that had the identical DNA composition to the G4 construct, but the Cy3 dye was relocated 18 or 6 nucleotides from the 5′ Cy5 dye (Figures 2A and 2B). If POT1 binds from the 3′ end, we expect a time delay prior to the first FRET decrease in the two alternate DNAs. If POT1 binds from the 5′ end, the FRET decrease should occur at about the same time in all three constructs. For this comparison, we measured the dwell time between the time of protein addition and the time of first FRET decrease. Figure 2C shows the representative traces from all three G4 substrates and the average dwell times analyzed from over 70 molecules. The substantially longer dwell times obtained for the alternate G4 constructs (Figure 2D) clearly indicate that POT1 selectively initiates binding from the 3′ end, likely due to a better accessibility of the overhang. Together, our data support a model in which one OB fold of monomeric POT1 binds G4, partially unfolding the G-quadruplex at the 3′ end, which allows the second OB fold to associate with the adjacent loop/repeat in the DNA. In this way, the four arms of G-quadruplex are expected to unfold sequentially one-by-one while POT1 binds from 3′ to 5′ direction, one OB fold at a time (Figure 2E).

To check if the stepwise binding and unfolding is specific to POT1, we used a single-stranded binding protein, gp32 from T4 bacteriophage and the G4 FRET construct. The gp32 protein exhibits a minimum binding size of seven nucleotides, which is comparable with POT1's ten nucleotide sequence requirement. In contrast to POT1, gp32 binding produced a one-step FRET decrease from 0.8 to 0.3, followed by dissociation. The protein binding and dissociation was observed as FRET fluctuations between 0.8 and 0.3 as indicated in the single molecule trace and transition density plot (Figure S2). Therefore, we conclude that the stepwise binding is specific to POT1.

POT1-TPP1N Induces Dynamic Folding and Unfolding of Telomeric Overhangs

To study how POT1-TPP1 complex interacts with the G-quadruplex folded overhang, we purified a well-characterized truncated form of TPP1, TPP1N, which retains the OB domains and stimulates POT1 binding to telomeric DNA and telomerase processivity (Wang et al., 2007). TPP1N consists of residues 87 to 334; however, the 87 N-terminal amino acids are functionally dispensable in human cells and are not conserved in orthologs from other organisms (Houghtaling et al., 2004; Liu et al., 2004; Ye et al., 2004). In addition, TPP1N retains interaction with POT1 and telomerase (Xin et al., 2007). We applied the preformed POT1-TPP1N (100 nM) complex to the same G4 DNA as used in POT1 binding (Figure 3A, top). We observed FRET decrease in two steps, which resembled the one POT1 monomer binding in which the two steps arise from OB1 and OB2 binding (compare Figure 3B top

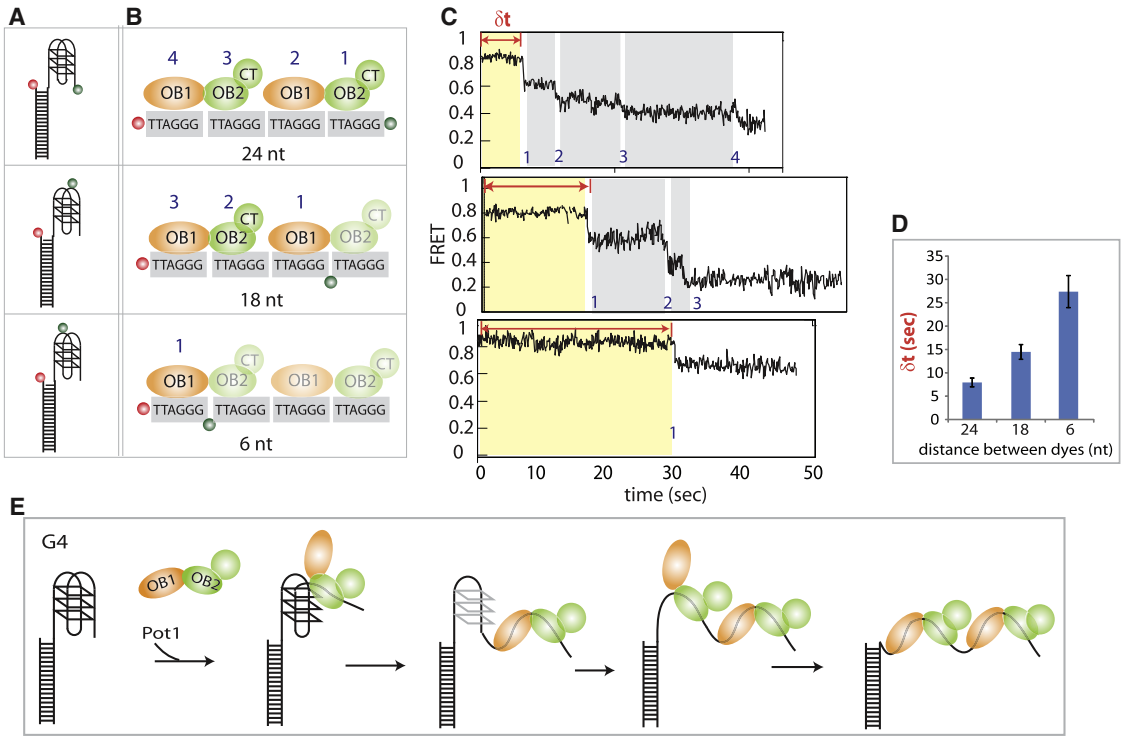

Figure 2. POT1 Binds Overhangs Directionally from 3′ to 5′

(A) Schematic of the G4 DNA with various dye positions.

(B and C) Schematic diagram representing the dye positions with respect to the individual OB fold binding sites. CT indicates C-terminal domain of POT1. The positions 24, 18, and 6 nt represent the distances between Cy3 and Cy5. The faint ovals indicate the OB unit bindings that should not induce FRET decrease. The step number shown in the single molecule traces (C) expected from individual OB fold binding is written above each oval. Single molecule traces obtained from the three DNA constructs (C). The δt indicates the time interval between POT1 addition and the first step of FRET decrease.

(D) The average δt from each DNA construct. The longest δt for the 6 nt DNA construct suggests POT1 binding initiates from the 3′ to 5′ direction. Error bars indicate the SEM.

(E) Schematic of a plausible POT1 binding mode.

See also Figure S2.

panel to Figure 1C bottom panel). Unlike the continuous stepwise FRET decrease seen in POT1 binding, we observed stable FRET for about 1–2 min, followed by fluctuation at mid- to low-FRET range, implying dynamic and continuous conformational changes within the telomeric overhang induced by the POT1-TPP1N complex (Figure 3B, top). To further characterize this behavior, we used three alternate FRET constructs, which had Cy3 to Cy5 distances of 18, 12, and 6 nt (Figure 3A). When the POT1-TPP1N complex was added to the 18 nt DNA, we observed one step of FRET decrease from high- to mid-level. The one-step FRET decrease is expected since the dye position is not sensitive to the first OB binding but only to the second OB binding. This was followed by FRET fluctuations, indicating dynamic folding and unfolding of G-quadruplex DNA, similar to the 24 nt construct, except at a higher FRET range due to the closer distance between the two dyes (Figure 3B, second panel). Such fluctuation is less prominent in the 12 and 6 nt DNA, likely due to a reduced degree of unfolding experienced in this region of DNA (Figure 3B, third and fourth panels). FRET histograms built from over 100 molecules show the overall FRET pattern in the three substrates tested (Figure 3C). To test if the FRET fluctuations arise from the same source, we measured dwell times (δt) from several hundred events obtained from the 24 and 18 nt substrates and plotted them as a histogram (Figure 3D). The similar dwell time distribution in both DNA constructs suggests that the dynamic fluctuation is not random, but arises from the same activity induced by POT1-TPP1N. The FRET pattern observed in the four constructs together indicates that the POT1-TPP1N complex generates dynamic folding and unfolding of the telomeric overhang DNA.

POT1-TPP1N Displays Dynamic Movement on Telomeric Overhangs

How does the POT1-TPP1N complex induce the conformational dynamics in the telomeric overhang? To address this question, we applied POT1 and fluorescently (Alexa 647) labeled TPP1N to the 3′ Cy3 labeled G4 construct to directly visualize the protein complex on the DNA substrate (Figure 4A, top). The labeling efficiency was approximately 65% as measured by absorbance spectrophotometer, and the presence of a single fluorophore on one protein was confirmed by the intensity level expected from a single dye and one-step photobleaching of Alexa 647 dye. This enables us to observe an individual POT1-TPP1N complex on a single DNA molecule. Here, we detected the

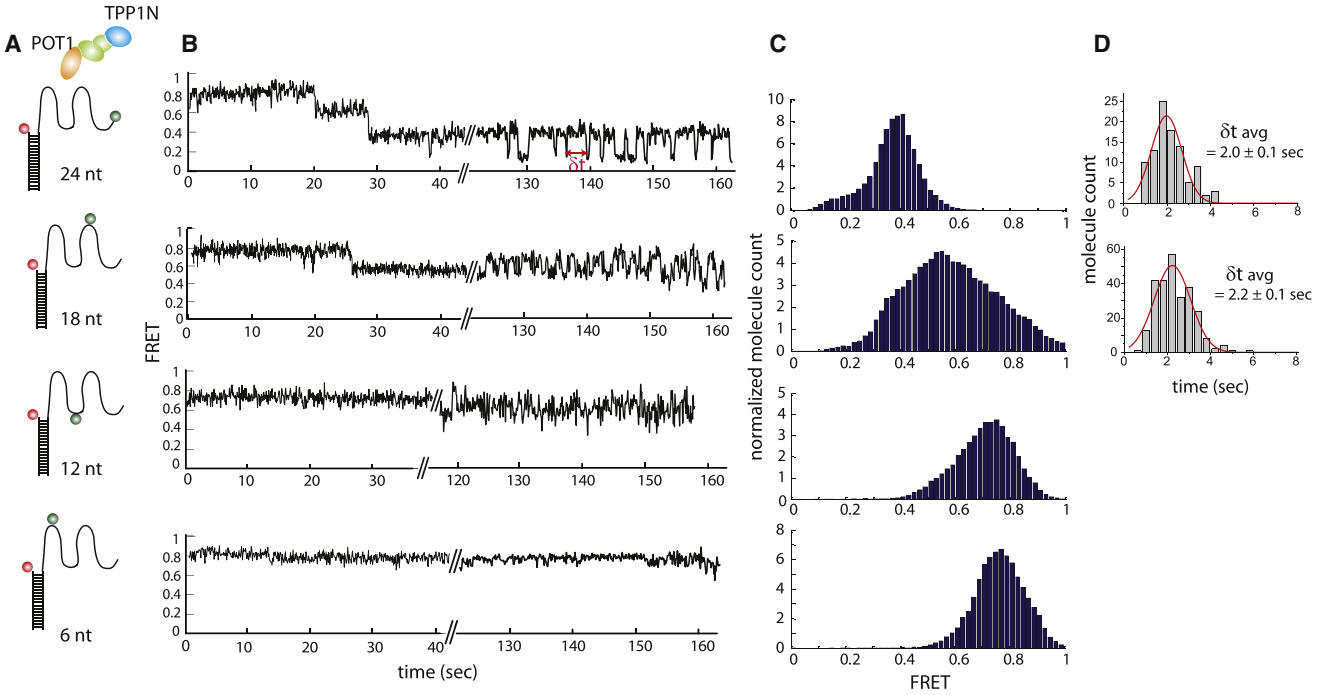

Figure 3. POT1-TPP1N Induces Folding-Unfolding Dynamics on Telomeric Overhangs

(A) Schematic of unlabeled TPP1N and POT1 on the G4 FRET construct with Cy3 dyes placed 24, 18, 12, and 6 nt from the duplex junction.

(B) Single molecule traces collected from all DNA substrates shows initial FRET decreases representing POT1-TPP1N binding by POT1 recognition of the telomeric overhang sequence, followed by continuous FRET fluctuations of the 24 and 18 nt DNA and less pronounced FRET changes for the other DNA constructs. We interpret the FRET fluctuations as dynamic folding and unfolding of G-quadruplex DNA induced by POT1-TPP1N.

(C) FRET histograms built from FRET values collected from 100 single molecule traces that exhibit dynamic folding-unfolding of unlabeled POT1-TPP1N on the G4 DNA FRET constructs.

(D) Dwell time histograms from over several hundred events of 24 and 18 nt G4 DNA FRET constructs.

See also Figure S3. Gaussian fit yields center of the histogram with the SEM.

binding of a POT1-TPP1N complex as an abrupt appearance of FRET, followed by continuous FRET fluctuation (Figure 4B, top). We note that the FRET fluctuation is not due to successive binding and unbinding events because the lowest FRET value is at 0.3–0.4, which is far above the value expected from dissociation of the protein (0.18). Therefore, we reason that the FRET fluctuations arise from a continuous association between the labeled protein and the 3′ terminus of the G4 DNA. This activity is specific to POT1-TPP1N since Alexa 647 labeled TPP1N added to G4 only shows an abrupt FRET increase and decrease reflecting a short binding period of TPP1N to G4. We also confirmed that fluorescence labeling does not perturb the protein activity by performing an alternative fluorescence assay, PIFE (Figure S3; Hwang et al., 2011). Unlike TPP1N, which only transiently associates with G4 (about 2.5 s averaged over 100 events), the POT1-TPP1N complex stays on the overhang for a substantially longer period (45 s averaged over 100 events). This is likely due to the behavior of the POT1-TPP1 complex, not individual protein, since POT1-TPP1 forms a stable complex when bound to telomere overhang DNA (Liu et al., 2004; Wang et al., 2007; Xin et al., 2007).

To further characterize this sliding effect, we subjected POT1-TPP1N (Alexa 647) to four alternate substrates, which have Cy3 dye located 18, 12, 6, and 0 nt away from the duplex junction (Figure 4A). Both the 24 and 18 nt DNA yield a robust FRET fluctuation exhibiting high- to low-FRET values, whereas the amplitude of FRET change is substantially reduced in the 12 and 6 nt DNA, with no detectable FRET change in the 0 nt substrate (Figures 4B and 4C). In light of the folding unfolding dynamics shown on the same DNA overhang (Figure 3B), the FRET fluctuation seen in the 24 and 18 nt constructs here is likely arising from POT1-TPP1N sliding back and forth on the G4 DNA. The more pronounced FRET changes seen in the 24 and 18 nt DNA compared to the other three substrates can be attributed to two sources. First, TPP1N (Alex 647) is expected to be positioned near the 3′ end of telomeric overhang since it interacts with the C-terminal region of POT1 near the POT1 OB2 fold (Liu et al., 2004; Ye et al., 2004), giving rise to the high FRET. Second, the activity of POT1-TPP1 may be more localized to the 3′ end, consistent with the more pronounced effect of folding and unfolding dynamics seen near the 3′ end (Figures 4A and 4B). In addition, the protein dwell times measured for the 24 and 18 nt DNA (Figure 4D) match closely to each other as well as to the folding unfolding kinetics of the DNA as shown in Figure 3D, strongly suggesting that this protein sliding motion is responsible for the folding and unfolding of G-quadruplex DNA.

POT1-TPP1N Slides on Mutant Telomeric Sequence

A previous study showed that POT1-TPP1N enhanced the telomerase processivity even on substrates that possessed

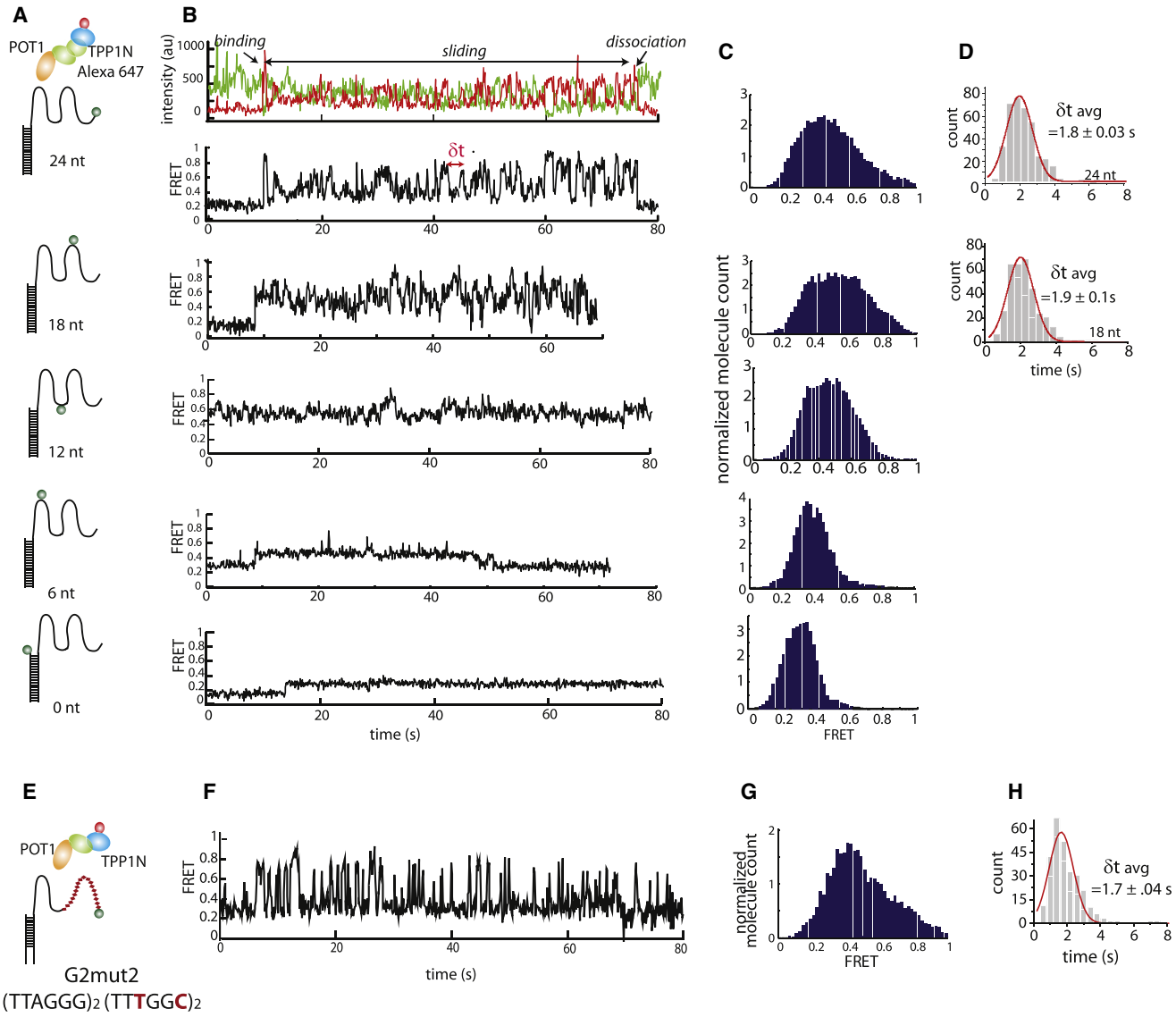

Figure 4. POT1-TPP1N Slides on the Telomeric Overhang near the 3′ End

(A) Schematic of Alexa 647-labeled TPP1N and POT1 on the G4 DNA construct, with the Cy3 dye located 24, 18, 12, 6, and 0 nt from the duplex junction.
(B) Single molecule traces show the initial FRET increase, followed by dynamic FRET fluctuations reflecting movement of POT1-TPP1N on the G4 DNA.
(C) FRET histograms taken from over 100 single molecule traces that display FRET fluctuation.
(D) Dwell times from several hundred events from the 24 and 18 nt G4 Cy3-DNA constructs. Gaussian fit yields center of the histogram with the SEM.
(E) Schematic of Alexa 647-labeled TPP1N and POT1 on the G2-mut2 DNA construct.
(F) Single molecule trace of POT1-TPP1N (Alexa 647) on G2-mut2 exhibits dynamic FRET fluctuations similar to the G4 DNA.
(G) FRET histogram built from over 100 single molecule traces that exhibit dynamic FRET fluctuation on the G2mut2 DNA.
(H) Dwell times from over several hundred events of sliding on the G2mut2 DNA construct.
See also Figures S4 and S5. Gaussian fit yields center of the histogram with the SEM.

modified telomeric sequence (Latrick and Cech, 2010). The mutant telomeric sequence had two telomeric repeats followed by multiple repeats of the mutated sequence "TTTGGC" (modified nucleotides are underlined). The mutant sequence allows binding and activity of telomerase harboring a mutant RNA template of the same sequence, but POT1-TPP1N cannot stably bind to the 3′ mutated repeats on the substrate. We hypothesized that POT1-TPP1's sliding movement may occur on this substrate and contribute to enhancing telomerase processivity. To test this, we adopted a sequence, which had two telomeric repeats followed by two repeats of the mutated sequence "TTTGGC," which we refer to as G2-mut2 (Figure 4E). First, we tested POT1 binding to the G2-mut2 construct. POT1 addition resulted in two steps of FRET decrease followed by a plateau at mid-FRET, indicating that only one POT1 monomer bound to the cognate sequence of two telomeric repeats, and the mutated sequence remained unbound by POT1 (Figures S4A and S4B). This is consistent with biochemical data that shows

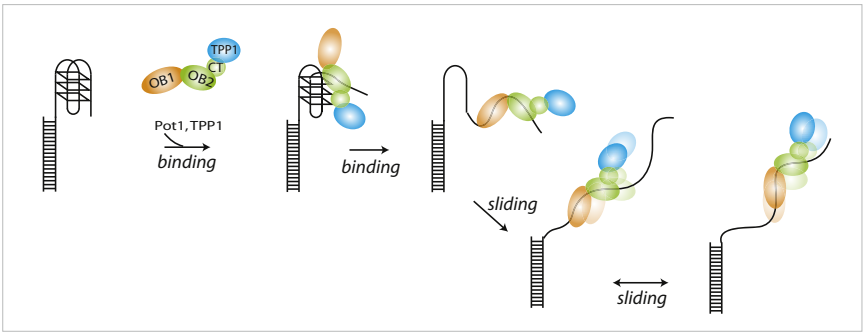

Figure 5. Proposed Mechanism of POT1-TPP1N Sliding
TPP1N-POT1 binds to the telomeric overhang from the 3′ end in a POT1-dependent manner and exhibits sliding clamp activity by diffusing along the telomeric overhang near the 3′ end.
See also Figure S5.

the mutant sequence does not allow POT1-TPP1 binding (Latrick and Cech, 2010).

Next, we added the POT1-TPP1N (Alexa 647) complex to the G2-mut2 DNA. Here, we observed FRET fluctuations analogous to the G4 construct, i.e FRET fluctuation exhibiting high- to low-levels (Figures 4F and 4G). The presence of high FRET in the single molecule trace indicates that POT1-TPP1N interacts with the mutant sequence situated at the 3′ region (Figure 4F). The range of FRET fluctuation and dwell time measured for this substrate (Figures 4G and 4H) are highly analogous to the pattern observed in the G4 substrate (Figures 4B and 4C, top), suggesting that the POT1-TPP1N complex slides back and forth on both substrates. Additionally, when we lengthened the mutant sequence to four repeats (G2-mut4), we still observed similar FRET fluctuation, albeit at a slightly reduced FRET value, strongly suggesting that POT1-TPP1N slides even on a longer stretch of the mutant sequence (Figures S4C–S4F). As a control measurement, we subjected POT1-TPP1N (Alexa 647) to a poly-thymidine (25 nt) substrate and observed no FRET fluctuation (Figures S5A and S5B). In addition, we substituted POT1 with gp32 (T4 bacteriophage gene product 32), which is an ssDNA binding protein that does not stimulate telomerase processivity (Latrick and Cech, 2010). In this case, we obtained FRET traces, which indicate binding and unbinding of TPP1N, but no FRET fluctuations resembling POT1-TPP1N sliding (Figures S5C and S5D). Therefore, we demonstrate that the dynamic sliding motion is specific to the POT1-TPP1N complex on telomeric overhang DNA and that POT1-TPP1 can slide even on the mutated telomere sequence to which POT1 cannot stably bind on its own. Taken together, we propose a sliding clamp model whereby the POT1-TPP1N slides back and forth on the telomeric overhang and thereby generates unfolding and folding dynamics near the 3′ region (Figure 5). In contrast to the sequential binding of POT1, which sequesters the overhang in an unfolded state, POT1-TPP1N presents a disparate mechanism involving a dynamic sliding movement.

DISCUSSION

The investigation of telomeric overhang DNA dynamics is complicated because bulk-phase ensemble studies cannot resolve transient protein-DNA interactions and inter- and intra-molecular dynamics. Single molecule approaches allow for the real time detection of nucleic acid structural dynamics as the substrate undergoes interaction with a protein and protein complexes. Unexpectedly, we observed a two-step binding process of one POT1 monomer to a telomeric overhang (Figures 1D and 1E). Based on the sequence specificity of POT1 binding to telomeric DNA (Lei et al., 2004), our results suggest that one OB fold binds one telomeric repeat at each step. The dwell time analysis, i.e the difference between 24 and 18 nt DNA (Figures 2C and 2D), indicates that the OB2 fold initiates unfolding of the G-quadruplex by binding to the TTAG nucleotides at the 3′ terminus, followed by the OB1 fold engaging with the second TTAGGG repeat, further unfolding the G-quadruplex (Figure 2E). Unlike other ssDNA binding proteins, such as RecA and Rad51, the POT1 structure reveals a sharp turn between the two OB fold domains, generating a sawtooth-like bending on the DNA (Lei et al., 2004). The sequential two-step binding of POT1 that we report here may explain how POT1 binding to the heavily structured telomeric DNA is facilitated by the two-step binding that results in a kinked domain arrangement.

The POT1-TPP1N interaction with telomeric G-quadruplex DNA revealed surprising dynamics, which is in striking contrast to the POT1 binding alone. Our data are consistent with the interpretation that the POT1-TPP1N complex slides back and forth on the overhang, generating G-quadruplex unfolding and refolding dynamics near the 3′ end of overhang, possibly contributing to the reduced protein-DNA FRET changes observed when the DNA dye was located near the 5′ side of the overhang, compared to its location near the 3′ end (Figure 4B). The same sliding motion occurred on an overhang containing mutant telomeric sequence at the 3′ end (Figures 4F and 4G), demonstrating that TPP1N alters the nature of POT1 interaction with telomeric DNA so as to impart mobility, even on the mutant sequence to which POT1 cannot bind by itself.

Based on our data, we postulate a mechanism in which the POT1-TPP1N complex engages with the telomeric sequence in a POT1 dependent manner and converts to a sliding clamp, which diffuses on the telomeric overhang (Figure 5). TPP1N lacks the interaction domain with TIN2, which tethers POT1-TPP1 to shelterin and the telomere (Takai et al., 2011). Thus, POT1-TPP1 (full length) sliding along ssDNA while tethered to duplex DNA via shelterin may generate an ssDNA loop as proposed previously (Latrick and Cech, 2010).

This sliding activity may partially explain the ability of POT1-TPP1N to enhance telomerase processivity, even on an overhang with mutant telomeric sequence. We hypothesize that the sliding motion of POT1-TPP1N may serve in this capacity in three ways. First, it may facilitate loading of telomerase at the 3′ terminus by making the 3′ end of the overhang accessible, i.e when the complex slides away from 3′ end, the 3′ tail is exposed to allow for telomerase loading. Second, the mobility of POT1-TPP1 near the 3′ tail may help to retain telomerase on the

telomeric overhang by continuously engaging with the telomerase. Third, the sliding activity may physically promote the propulsion of the telomerase, thereby enhancing its translocation along the telomeric overhang. The ability of the POT1-TPP1N complex to slide along ssDNA may be highly analogous to the proliferating cell nuclear antigen sliding clamp, which greatly enhances the processivity of DNA polymerases (Bowman et al., 2004).

EXPERIMENTAL PROCEDURES

Buffers

G2, G3, and G4 salt titration buffers consisted of either 0–100 mM KCl or 0–150 mM NaCl in 25 mM Tris (pH8). POT1 reaction buffer contained 150 mM NaCl in 25 mM Tris pH 8. For single molecule imaging, 0.8 mg/ml glucose oxidase, 0.625% glucose, ~3 mM 6-hydroxy-2,5,7,8-tetramethylchromane-2-carboxylic (Trolox), and 0.03 mg/ml catalase were added to the buffers.

DNA Constructs

Oligonucleotides required to make the partial DNA duplex substrates were purchased from IDT with either Cy3 or Cy5 dyes (Table 1). The G3 construct was purchased with an amino modifier C6 dT at the 3′ end and reacted with NHS-ester conjugated Cy3 (GE Healthcare). Briefly, 10 mM dye was incubated with 0.15 mM DNA in 100 mM sodium tetraborate pH 8.5 buffer overnight. The excess dye was then filtered out using Micro Bio-spin 6 column (Biorad) twice.

Telomeric DNA constructs were prepared by mixing a 3′Cy3 sequence with the 3′ biotin sequence at a molar ratio of 1:1.5 in 20 mM Tris-HCl pH 7.5, 50 mM NaCl and incubating at 95°C for 2 min then slowly cooling to room temperature for 2 hr.

POT1 and TPP1N Protein Purification

Recombinant human POT1 protein was purified using a baculovirus/insect cell expression system as described previously (Sowd et al., 2008). The hexahistidine Sumo-tagged TPP1N (amino acids 89–334) construct was kindly provided by Dr. Ming Lei (University of Michigan). Expression was induced with 0.1 mM isopropyl 1-thio-β-D-galactopyranoside in *Escherichia coli* BL21 (DE3) pLysS cells, and the protein was purified as previously described (Sowd et al., 2009).

Fluorescent Labeling of TPP1N

The Alexa647 (NHS ester) was reacted with TPP1N in a 1:20 protein-dye ratio for 1 hr in 100 mM sodium bicarbonate buffer, pH 8.5. Excess dye was removed using a Micro Bio-spin 6 column (BioRad) twice.

Single Molecule Fluorescence Data Acquisition

Single molecule fluorescence experiments were carried out on quartz slides (Finkenbeiner). To minimize surface interactions with the protein, quartz slides and coverslips were coated with polyethylene glycol (PEG) (Roy et al., 2008). Briefly, the slides and coverslips were cleaned and treated with methanol, acetone, potassium hydroxide, burned, treated with aminosilane, and coated with a mixture of 97% mPEG (m-PEG-5000, Laysan Bio, Inc.) and 3% biotin PEG (biotin-PEG-5000, Laysan Bio, Inc).

Partial duplex DNA molecules were annealed and immobilized on the PEG-passivated surface via biotin-neutravidin interaction. Excess donor molecules were washed away with reaction buffer and supplemented with an oxygen scavenging system (0.8 mg/ml glucose oxidase, 0.625% glucose, ~3 mM 6-hydroxy-2,5,7,8-tetramethylchromane-2-carboxylic (Trolox), and 0.03 mg/ml catalase). Imaging was initiated before protein (POT1, TPP1N, or POT-TPP1N) was flowed through to capture the moment of protein binding to DNA. All experiments and measurements were carried out at room temperature (23°C ± 1°C).

Prism type total internal reflection microscopy was used to acquire single molecule FRET and PIFE data. A 532-nm Nd:YAG laser was guided through a prism to generate an evanescent field of illumination. A water-immersion objective was used to collect the signal and a 550-nm long pass filter was used to remove the scattered light. Cy3 signals were collected using a 630-nm dichroic mirror and sent to a charge-coupled device camera. Data were recorded with a time resolution of 100 ms as a stream of imaging frames and analyzed with scripts written in interactive data language to give fluorescence intensity time trajectories of individual molecules.

smFRET Data Analysis

Basic data analysis was carried out by scripts written in Matlab, with FRET efficiency, E, calculated as the intensity of the acceptor channel divided by the sum of the donor and acceptor intensities. Histograms were generated using over 6,000 molecules collected and were fit to Gaussian distributions using Origin 8.0, with the peak position left unrestrained. Fluorescence resonance energy transfer TDP are two-dimensional contour maps plotted from transitions collected from 200–800 FRET transitions. TDP is constructed by plotting values for each transition based upon FRET value from which the transition originated (y axis) to which FRET value the transition ends (x axis). Dwell times were collected by measuring the time the molecule spends in a particular FRET state. The means and the standard errors were plotted. Software for analyzing single-molecule FRET data is available for download from https://physics.illinois.edu/cplc/software/.

SUPPLEMENTAL INFORMATION

Supplemental Information includes five figures and can be found with this article online at http://dx.doi.org/10.1016/j.str.2012.08.018.

ACKNOWLEDGMENTS

The authors thank Brian Freeman and Ruobo Zhou for careful review of the manuscript, members of the Myong and Opresko laboratory for helpful discussions, and M. Lei for the TPP1N plasmid construct. Support for this work was provided by the American Cancer Society (Research Scholar Grant; RSG-12-066-01-DMC), the Human Frontier Science Program (RGP0007/2012), and the U.S. National Science Foundation Physics Frontiers Center Program (0822613) through Center for the Physics of Living Cells for S.M.; the Linda Su-Nan Chang Sah Doctoral Fellowship for H.H.; and NIH Grant ES0515052 and the David Scaife Foundation grant to the Center for Nucleic Acid Science and Technology for P.O. H.H. labeled the TPP1N protein, conducted all of the experiments, and analyzed all of the data. N.B. purified all of the proteins. S.M. performed experiment design, analyses, and interpretation of the data. S.M. wrote the manuscript, and P.O. contributed to writing the manuscript.

Received: May 14, 2012
Revised: August 13, 2012
Accepted: August 14, 2012
Published online: September 13, 2012

REFERENCES

Abreu, E., Aritonovska, E., Reichenbach, P., Cristofari, G., Culp, B., Terns, R.M., Lingner, J., and Terns, M.P. (2010). TIN2-tethered TPP1 recruits human telomerase to telomeres in vivo. Mol. Cell. Biol. *30*, 2971–2982.

Armanios, M., Alder, J.K., Parry, E.M., Karim, B., Strong, M.A., and Greider, C.W. (2009). Short telomeres are sufficient to cause the degenerative defects associated with aging. Am. J. Hum. Genet. *85*, 823–832.

Baumann, P., and Cech, T.R. (2001). Pot1, the putative telomere end-binding protein in fission yeast and humans. Science *292*, 1171–1175.

Bowman, G.D., O'Donnell, M., and Kuriyan, J. (2004). Structural analysis of a eukaryotic sliding DNA clamp-clamp loader complex. Nature *429*, 724–730.

d'Adda di Fagagna, F., Reaper, P.M., Clay-Farrace, L., Fiegler, H., Carr, P., Von Zglinicki, T., Saretzki, G., Carter, N.P., and Jackson, S.P. (2003). A DNA damage checkpoint response in telomere-initiated senescence. Nature *426*, 194–198.

Denchi, E.L., and de Lange, T. (2007). Protection of telomeres through independent control of ATM and ATR by TRF2 and POT1. Nature *448*, 1068–1071.

Gilbert, D.E., and Feigon, J. (1999). Multistranded DNA structures. Curr. Opin. Struct. Biol. *9*, 305–314.

Hockemeyer, D., Sfeir, A.J., Shay, J.W., Wright, W.E., and de Lange, T. (2005). POT1 protects telomeres from a transient DNA damage response and determines how human chromosomes end. EMBO J. *24*, 2667–2678.

Houghtaling, B.R., Cuttonaro, L., Chang, W., and Smith, S. (2004). A dynamic molecular link between the telomere length regulator TRF1 and the chromosome end protector TRF2. Curr. Biol. *14*, 1621–1631.

Hwang, H., Kim, H., and Myong, S. (2011). Protein induced fluorescence enhancement as a single molecule assay with short distance sensitivity. Proc. Natl. Acad. Sci. USA *108*, 7414–7418.

Kelleher, C., Kurth, I., and Lingner, J. (2005). Human protection of telomeres 1 (POT1) is a negative regulator of telomerase activity in vitro. Mol. Cell. Biol. *25*, 808–818.

Latrick, C.M., and Cech, T.R. (2010). POT1-TPP1 enhances telomerase processivity by slowing primer dissociation and aiding translocation. EMBO J. *29*, 924–933.

Lei, M., Podell, E.R., and Cech, T.R. (2004). Structure of human POT1 bound to telomeric single-stranded DNA provides a model for chromosome end-protection. Nat. Struct. Mol. Biol. *11*, 1223–1229.

Liu, D., Safari, A., O'Connor, M.S., Chan, D.W., Laegeler, A., Qin, J., and Songyang, Z. (2004). PTOP interacts with POT1 and regulates its localization to telomeres. Nat. Cell Biol. *6*, 673–680.

Makarov, V.L., Hirose, Y., and Langmore, J.P. (1997). Long G tails at both ends of human chromosomes suggest a C strand degradation mechanism for telomere shortening. Cell *88*, 657–666.

Murphy, M.C., Rasnik, I., Cheng, W., Lohman, T.M., and Ha, T. (2004). Probing single-stranded DNA conformational flexibility using fluorescence spectroscopy. Biophys. J. *86*, 2530–2537.

Neidle, S., and Parkinson, G.N. (2003). The structure of telomeric DNA. Curr. Opin. Struct. Biol. *13*, 275–283.

Roy, R., Hohng, S., and Ha, T. (2008). A practical guide to single-molecule FRET. Nat. Methods *5*, 507–516.

Sowd, G., Lei, M., and Opresko, P.L. (2008). Mechanism and substrate specificity of telomeric protein POT1 stimulation of the Werner syndrome helicase. Nucleic Acids Res. *36*, 4242–4256.

Sowd, G., Wang, H., Pretto, D., Chazin, W.J., and Opresko, P.L. (2009). Replication protein A stimulates the Werner syndrome protein branch migration activity. J. Biol. Chem. *284*, 34682–34691.

Sundquist, W.I., and Klug, A. (1989). Telomeric DNA dimerizes by formation of guanine tetrads between hairpin loops. Nature *342*, 825–829.

Takai, K.K., Kibe, T., Donigian, J.R., Frescas, D., and de Lange, T. (2011). Telomere protection by TPP1/POT1 requires tethering to TIN2. Mol. Cell *44*, 647–659.

Veldman, T., Etheridge, K.T., and Counter, C.M. (2004). Loss of hPot1 function leads to telomere instability and a cut-like phenotype. Curr. Biol. *14*, 2264–2270.

Wang, F., Podell, E.R., Zaug, A.J., Yang, Y., Baciu, P., Cech, T.R., and Lei, M. (2007). The POT1-TPP1 telomere complex is a telomerase processivity factor. Nature *445*, 506–510.

Williamson, J.R., Raghuraman, M.K., and Cech, T.R. (1989). Monovalent cation-induced structure of telomeric DNA: the G-quartet model. Cell *59*, 871–880.

Xin, H., Liu, D., Wan, M., Safari, A., Kim, H., Sun, W., O'Connor, M.S., and Songyang, Z. (2007). TPP1 is a homologue of ciliate TEBP-beta and interacts with POT1 to recruit telomerase. Nature *445*, 559–562.

Ye, J.Z., Hockemeyer, D., Krutchinsky, A.N., Loayza, D., Hooper, S.M., Chait, B.T., and de Lange, T. (2004). POT1-interacting protein PIP1: a telomere length regulator that recruits POT1 to the TIN2/TRF1 complex. Genes Dev. *18*, 1649–1654.

